

REGULATION OF THE INTERACTION OF INOSINE MONOPHOSPHATE DEHYDROGENASE WITH MYCOPHENOLIC ACID BY GTP

YanShan Ji^{*†}, JingJin Gu^{*†}, Alexander M. Makhov[‡], Jack D. Griffith[‡] and Beverly S. Mitchell^{*†}

From the Departments of Pharmacology^{*}, Medicine[†], Microbiology/Immunology[‡], and The Lineberger Comprehensive Cancer Center, University of North Carolina, Chapel Hill, North Carolina, 27599-7295

Running Title: GTP and IMPDH Inhibition by MPA

Address correspondence to: Beverly S. Mitchell, Departments of Pharmacology and Medicine, Lineberger Comprehensive Cancer Center, University of North Carolina, Chapel Hill, NC 27599-7295; Phone: 919-843-7710; Fax: 919-966-8212; E-Mail: mitchell@med.unc.edu

Inosine monophosphate dehydrogenase (IMPDH), a rate-limiting enzyme in the *de novo* synthesis of guanine nucleotides, is a major therapeutic target. A prototypic uncompetitive inhibitor of IMPDH, mycophenolic acid (MPA), is the active form of mycophenolate mofetil (CellCept[®]), a widely used immunosuppressive drug. We have found that MPA interacts with intracellular IMPDH *in vivo* to alter its mobility on SDS-polyacrylamide gels. MPA also induces a striking conformational change in IMPDH protein in intact cells, resulting in the formation of annular aggregates of protein with concomitant inhibition of IMPDH activity. These aggregates are not associated with any known intracellular organelles and are reversible by incubating cells with guanosine, which repletes intracellular GTP, or with GTP γ S. GTP also restores IMPDH activity. Treatment of highly purified IMPDH with MPA also results in the formation of large aggregates of protein, a process that is both prevented and reversed by the addition of GTP. Finally, GTP binds to IMPDH at physiologic concentrations, induces the formation of linear arrays of tetrameric protein, and prevents the aggregation of protein induced by MPA. We conclude that intracellular GTP acts as an antagonist to MPA by directly binding to IMPDH and reversing the conformational changes in the protein.

Inosine Monophosphate Dehydrogenase (IMPDH) catalyzes the first step in the *de novo* synthetic pathway for the formation of guanine nucleotides by converting IMP to XMP with the concomitant reduction of NAD⁺. As the rate-limiting step in this pathway, the enzyme has been identified as an important regulator of cell proliferation. Inhibitors of IMPDH are in clinical use as immunosuppressive agents and have potential utility in the treatment of neoplastic and viral diseases (1-5). Two isoforms of IMPDH have been identified, the type I form that is expressed at lower levels in all cell types and the type II form that is more highly expressed in proliferating and transformed cell types (6,7). These enzymes have 84% amino acid identity and both are catalytically active as tetramers of 55 kDa subunits with similar, although not identical, kinetic profiles.

Studies on the regulation of IMPDH activity have demonstrated strong transcriptional up-regulation of the type II mRNA in response to mitogenic stimuli in peripheral blood lymphocytes and in response to enzyme inhibition and guanine nucleotide depletion in a number of cell types (8,9). Until recently, very little attention has been paid to the role of protein structure in regulating its activity. The finding that mutations within the IMPDH type I coding region are associated with a familial form of retinitis pigmentosa (10) has initiated renewed interest in the structure of IMPDH, first crystallized in 1996 (11). These mutations occur within a region of the protein

termed the cystathione β -synthase (CBS) domain that has recently been shown to bind oligonucleotides up to 100 base pair in length (12). In addition, this domain binds ATP, resulting in allosteric activation of the enzyme (13). It has thus been postulated that IMPDH may act as an energy sensor in cells and have a more complex role in cellular physiology than previously imagined.

In investigating the potential of IMPDH inhibitors as antineoplastic drugs, we have discovered that these inhibitors induce macroaggregates of IMPDH protein that are reversible by the addition of GTP and to a lesser extent by ATP. More spectacularly, most aggregates take the form of ring structures in the cytoplasm of intact normal and neoplastic cells that regress with the repletion of intracellular guanine nucleotides. The unique nature of this protein self-association may account in part for the effects of IMPDH inhibitors and suggest that intracellular levels of GTP may regulate the interaction of IMPDH with small molecule inhibitors.

EXPERIMENTAL PROCEDURES

Cell Culture and Treatment Conditions — The human breast cancer cell line MCF7 was cultured in DMEM medium supplemented with 10% heat-inactivated fetal bovine serum and 100 μ g/ml penicillin and streptomycin. The human acute lymphoblastic leukemia cell line CEM and hypoxanthine-guanine phosphoribosyl transferase (HGPRT)-deficient hybridoma K6H6/B5 cells (ATCC, Manassas, VA) were cultured in RPMI 1640 medium with the same supplements. HGPRT-deficient CEM cells were maintained in 5 μ g/ml 6-thioguanine (6-TG) in RPMI 1640 medium with supplements.

Mycophenolic acid (Sigma, St Louis, MO) was solubilized in ethanol and used at a final concentration of 2 μ M. Equal volumes of ethanol were added to all untreated controls. Guanosine was added to a final concentration of 100 μ M. GTP and non-hydrolysable GTP γ S (Sigma) were used at 1 mM.

Leukemic Cell Isolation and Western Blots— Peripheral blood samples were obtained from a patient with chronic myelogenous leukemia (CML) treated with CellCept[®], an ester pro-drug

of MPA, and a normal volunteer. Mononuclear cells were separated using Histopaque-1077 (Sigma). The cells were lysed by 3 freeze-thaw cycles in an extraction buffer containing 200 mM Tris-HCl, pH7.5; 200 mM NaCl; 10% glycerol; 2 mM DTT; 5 mM MgCl₂; 1 mM EGTA; 2 μ g/ml of leupeptin and pepstatin; and 0.1 mM PMSF. Total lysates (10 μ g) were run on a 15% SDS-polyacrylamide gel. The Western blot was probed using a polyclonal antibody kindly provided by Vertex (Cambridge, MA).

IMPDH Activity Assay — The enzymatic activity of IMPDH was measured by the increase in absorbance at 290 nm (formation of XMP) in crude cell extracts or at 340 nm (formation of NADH) for purified IMPDH at 37°C. The assay buffer was pre-warmed to 37°C and contained 100 mM Tris/HCl, pH 8.0, 100 mM KCl, 50 μ g/ml BSA, 1 mM DTT, 2 mM EDTA, 5 mM MgCl₂, 200 μ M IMP, 200 μ M NAD⁺. The activities from 40 μ l of whole cell extracts or 5 μ g of purified IMPDH were recorded over 10 min after adding 1 ml of assay buffer by a temperature-controlled UV-visible recording spectrophotometer UV160U (Shimadzu Co., Kyoto, Japan). The amount of protein was determined by Bradford protein assay and the activity is expressed as nmol/min/mg protein.

Immunohistochemical and Electron Micrograph Analysis of IMPDH — MCF7 cells were cultured on cover slips in 12-well plate in the absence or presence of 2 μ M MPA and the indicated additives. Cells were fixed for 15 min in 1ml of 4% paraformaldehyde (Electron Microscopy Sciences, Hatfield, PA) followed by treatment with 0.2% Triton X-100 for 5 min. After 30 min blocking, the cells were incubated with 100 μ l rabbit anti-IMPDH Ab diluted 1:300 in 50% blocking solution (2% FBS, 2% BSA, 2% normal goat and rabbit serums in PBS) for 1 h at RT. The cells were then incubated with FITC-labeled goat-anti-rabbit conjugates diluted 1:300 in 50% blocking solution for 1 h, washed 3 times with PBS, and mounted with Vectorshield (Vector, Peterborough, UK) for fluorescent and confocal microscopy.

For immunogold staining and electron microscopy, cells were fixed with 1% glutaraldehyde and blocked with 1% BSA in PBS for 30 min. The IMPDH Ab in 1% BSA was

incubated with cells for 1 h, and the cells were washed and incubated with 1:200 NANOGOLD[®] reagent (Nanoprobe Inc., Yaphank, NY) for 1 h at RT. Cells were post-fixed with 1% glutaraldehyde. The nanogold particles were then silver-enhanced using a HQ Silver Enhancement Kit (Nanoprobe Inc.) according to the manufacturer's instruction. The ultra-thin sections were stained with lead-citrate solution and were examined by a Philips CM12 transmission electron microscope.

Gel Filtration of Proteins with FPLC — MCF7 cells cultured with 2 μ M MPA for 6 h were harvested and briefly sonicated on ice in PBS containing 100 mM KCl, 1 mM DTT, 0.1% Tween 20, and protease inhibitor cocktail. The whole cell extracts were clarified by centrifugation at 14,000 rpm for 20 min and applied to a Sephacryl S-500 column connected to a FPLC system (Amersham Biosciences). Fractions were collected at a flow rate of 12 ml/h. Equal volumes of proteins from each fraction were resolved by SDS-PAGE and immunoblotted using anti-IMPDH specific Ab. The relative protein levels of IMPDH were quantitated by a densitometer. Protein standards (Sigma) were applied to the same column to generate a standard curve, from which the molecular masses for IMPDH and its aggregates were calculated.

Recombinant Human IMPDH Purification and Treatment in Vitro — To facilitate purification, the type II IMPDH cDNA was cloned into the pET-24C vector and transformed into *Escherichia coli* BL21 (DE3). After induction with isopropyl thiogalactoside, the cell pellets were resuspended in 1X binding buffer (Invitrogen, Carisbad, CA) containing 5mM DTT, 1 mg/ml lysozyme and EDTA-free protease inhibitor cocktail. Following sonication on ice and centrifugation at 25,000g for 20 min at 4°C, the His-tagged IMPDH II proteins were purified on a Ni-NTA column (Invitrogen). Fractions were collected using a 50 mM to 200 mM imidazole gradient elution and were dialyzed with buffer containing 50 mM HEPES, pH 7.9, and 100 mM KCl. Glycerol was added to a final concentration of 20% and the samples were stored at -20°C.

For *in vitro* treatment, the purified IMPDH was further diluted to a final concentration of 0.1 mg/ml and 2 μ M MPA was added for 15 min at RT. IMPDH proteins were spread on poly-lysine

coated glass slides, stained using the immunohistochemical staining procedure, and visualized by fluorescent microscopy at a magnification of 1000x. Purified IMPDH was also prepared for EM at a final concentration of 50 μ g/ml in HEPES buffer. After treatment with nucleotides, MPA, or the combination, each sample was mounted on glow charged thin carbon foils, and stained with 2% uranyl acetate (14). Micrographs were taken on a Philips CM12 electron microscope at 80 kV and a magnification of 45,000x.

GTP binding assay — Binding of GTP to purified IMPDH was determined with a rapid filtration technique (13,15). 1.0 μ M of [α -³²P]GTP was mixed with increasing concentrations of cold GTP and incubated with 0.25 μ M (55 μ g/ml) IMPDH for 10 min at RT in 20 μ l of reaction buffer containing 50 mM Tris-HCl, pH 8.0, 150 mM KCl, 2.5 μ M BSA. Non-specific control values were obtained under the same conditions substituting BSA for IMPDH. 10 μ l of the reaction mixture were loaded on a Millipore MF Filter Membrane (Millipore Corp) rapidly under vacuum and washed with 1 ml of ice-cold reaction buffer. Radioactivity on the filters was measured by scintillation counting and data were plotted using SigmaPlot (SYSTAT, CA).

RESULTS

Effect of MPA on IMPDH Protein — To study the direct effect of MPA on IMPDH protein, we performed Western blot analysis of IMPDH following MPA treatment. In MCF7 cells, a distinct decrease in the mobility of IMPDH occurred within 5 min of MPA addition (Fig. 1A, lane 3). The addition of guanosine, which restores guanine nucleotide pools through the HGPRT salvage pathway, completely prevented this band shift (Fig. 1A, lane 2). Approximately 50% of the protein migrated more slowly and the amount of protein shifted did not change with increased time of incubation with drug (Fig. 1A, lanes 4 and 5). A similar shift has previously been reported for the yeast protein (16). Importantly, this shift was also observed for human IMPDH obtained from the mononuclear cells of a patient treated with immunosuppressive doses of CellCept[®], an ester pro-drug of MPA (Fig. 1B). The addition of

guanosine with MPA completely prevented the shift, while guanosine treatment for the last 10 min slightly reduced the shift (Fig. 1C, lane 3 and 4). The shifted band disappeared after withdrawal of MPA (Fig. 1C, lane 5), reflecting the rapid metabolism of the bound MPA by glucuronidation (17,18). IMPDH activity in MCF7 cells treated with 2 μ M MPA for 24 h was decreased by about 50% (Fig. 1D); this inhibition was completely reversed by the addition of guanosine for 60 min. The changes in activity of IMPDH following MPA treatment correlate with the amount of protein shifted on Western blots.

Aggregation of IMPDH Protein by MPA Treatment in Intact Cells —We then examined the effect of MPA treatment on intracellular IMPDH distribution by immunofluorescent staining. As shown in Figure 2A, IMPDH is located diffusely in the cytosolic compartment in untreated cells. Within 30 min of MPA treatment, IMPDH protein started to form elongated structures. Within 24 h, we observed a striking aggregation of the protein into perinuclear linear arrays more than 10 microns in length and subsequently into clearly defined annular configurations. This aggregation was seen in all cell lines examined, including a number of leukemic and solid tumor cell lines, as well as in normal peripheral blood lymphocytes. Using laser powered confocal microscopy, we examined the shape of the aggregates in greater detail. As shown in Figure 2B, there was a marked predominance of ring formations. Finally, we examined the structures using high resolution electron microscopy with immunogold staining of IMPDH in MCF7 cells (Fig. 2C). After silver enhancement, the nanogold staining again demonstrated IMPDH organized into large linear or circular arrays in the cytoplasm. Of particular note is the fact that IMPDH is not associated with any organelles or other defined intracellular structures by this high resolution technique. In other studies, we did not find co-localization of mitochondria, golgi apparatus, endoplasmic reticulum, lipid bodies or cytokeratins with IMPDH by light microscopy (data not shown). In addition, extensive co-immunoprecipitation experiments and tandem affinity purification using tagged IMPDH did not demonstrate any interacting protein other than endogenous IMPDH.

Reversal of IMPDH Aggregates by GTP — We then tested whether guanosine reverses IMPDH

aggregation by repleting guanine nucleotide pools. MPA-induced IMPDH aggregates are reversed within 1 h by adding 100 μ M guanosine to MCF7 cells cultured for 24 h in the presence of 2 μ M MPA (Fig. 3C). In data not shown, the addition of equivalent concentrations of guanine, GMP, GDP or GTP were equally effective in reversing aggregation, while the addition of NAD⁺, PRPP, xanthine, hypoxanthine, adenosine, AMP, ADP or ATP had no effect in either MCF7 or CEM cells. We then asked whether the intracellular HGPRT salvage pathway that converts guanine to GMP is necessary for this effect. Guanosine is metabolized to guanine by the enzyme purine nucleoside phosphorylase that is present in fetal bovine serum. The use of HGPRT-deficient cells enabled us to determine whether either guanosine or guanine had a direct effect on IMPDH aggregation, or whether they were acting through conversion into guanine nucleotides. As shown in Figure 3A and B, guanosine was unable to reverse the IMPDH aggregates in HGPRT-deficient CEM and K6H6/B5 cells. However, the addition of 1 mM GTP resulted in complete dispersal. This result is surprising in that there is no well-defined mechanism for the transport of GTP directly from the extracellular to the intracellular compartment. Therefore, these results were confirmed by adding GTP γ S, a non-hydrolysable GTP analog, to MPA treated MCF7 cells. The aggregates dispersed, with the subsequent appearance of IMPDH in nucleoli, as well as diffusely within the cytoplasm within 60 min (Fig. 3C). Subsequent experiments using [³⁵S]GTP γ S confirmed that the nucleotide is able to get across the MCF7 plasma membrane in a time-dependent and dose-dependent manner (data not shown). These results confirm that guanosine reverses the MPA-induced IMPDH aggregates through salvage to guanine nucleotides and that GTP is the direct effector. The structural changes in IMPDH correlate with changes of activity. The approximate 50% reduction in activity induced by MPA was completely reversed by the addition of 1 mM GTP γ S to cells for one hour (Fig. 3D). These data indicate that increasing the intracellular GTP level overcomes the inhibition of IMPDH induced by MPA.

IMPDH aggregation induced by MPA—To further define IMPDH aggregation, the distribution of IMPDH in control or MPA treated cell extracts

was examined using a Sephacryl S-500 size exclusion column (Fig. 4A). Treatment of MCF7 cells with MPA for 6 h resulted in an increase in the size of the IMPDH complex, as detected by Western blot of IMPDH monomers, from a peak of 400 kDa to a peak of 600 kDa with sizes ranging upwards of 2,000 kDa and extending into the void volume. These data support the view that MPA promotes self-aggregation of IMPDH protein and that the higher molecular weight multimers are in equilibrium (11,19). Further support for this concept comes from studies on purified recombinant IMPDH type II. His-tagged IMPDH II expressed in *E. coli* was purified to homogeneity. The protein was treated with MPA, spread on poly-lysine coated glass slides and visualized using standard immunofluorescence microscopy (Fig. 4B). Treatment with MPA results in the formation of large aggregates with a tendency to annular formation, although without the same level of definition found in intact cells. These data demonstrate that MPA causes self-aggregation of IMPDH in the absence of other proteins or cellular elements, most likely through conformational change (20).

Effect of GTP on IMPDH in Vitro—To examine the molecular sequelae of both MPA-induced and GTP-induced changes on the purified protein, we performed uranyl acetate negative staining of protein followed by electron microscopic examination (Fig. 5). This technique allows visualization of IMPDH homotetramers that are 14.6 ± 0.9 nm (N=10) in diameter. Protein treated only with ethanol exists predominantly as single or ditetrameric units (panel A). MPA treatment for 15 min resulted in the formation of large aggregates of the tetramer ranging in size from 0.1 μ m to more than 1 μ m in diameter (Panel D). These aggregates are stable in solution over time at room temperature. The addition of 1 mM GTP alone to IMPDH protein in solution resulted in the formation of linear arrays consisting of IMPDH tetramers (Panel B). GTP reversed the IMPDH aggregates formed as a consequence of MPA exposure (Panel E), again resulting in linear arrays. ATP, an allosteric activator of IMPDH (13), also increased the formation of linear IMPDH chains (Panel C) and reduced the size of MPA-induced aggregates (Panel F), although neither effect was as pronounced as that caused by GTP. Both GTP and ATP at 1-2 mM

concentrations increased the activity of purified IMPDH by about 20% (data not shown). Neither CTP nor UTP had any effect on IMPDH alone or in the presence of MPA (not shown). MPA treatment did not induce protein aggregation after pre-incubation with GTP or ATP, but did with CTP or UTP (data not shown). These results are summarized in Figure 6.

IMPDH Binding of GTP—Although it has recently been demonstrated that the CBS domains of IMPDH can bind ATP (13), GTP binding has not been demonstrated. Figure 7 shows that GTP binds to purified IMPDH protein, albeit with low affinity. Data were fitted to a four parameter logistic curve using SigmaPlot. The apparent K_d is 72.9 ± 8.1 μ M, which is within the physiologically relevant range. This binding also displays positive cooperativity, with a Hill slope of 1.7.

DISCUSSION

IMPDH has long been considered to be an important pharmacologic target and a number of inhibitors have been developed and used in preclinical studies (21,22). Of these, three are in widespread clinical use. Ribavirin, a broad spectrum antiviral agent used in the treatment of Hepatitis C in combination with interferon- α , is a relatively weak IMPDH inhibitor (23). Mizoribine (Bredinin) and Mycophenolate mofetil (CellCept) are used as immunosuppressive agents in the setting of organ transplantation, graft-versus-host disease and vasculitis in Japan and the United States, respectively (24). Given the clinical importance of IMPDH as a drug target, the enzyme has been crystallized from a number of species and the structural basis of its inhibition has been examined in detail as the basis for new drug design (11,25,26).

Human IMPDH is a tetramer of 55 kDa subunit consisting of α/β barrels, with the active site located at the monomer-monomer interface. The catalytic site is a α/β barrel of approximately 400 residues. The substrate (IMP) and cofactor (NAD^+) bind in a continuous cleft on the C-terminal face of each barrel (25). The oxidation of IMP to XMP proceeds through a covalent mechanism involving an active site cysteine residue. The uncompetitive inhibitor MPA binds directly at the NAD^+ site and traps the XMP as a

covalent intermediate in an open configuration of the enzyme. Mizoribine, in contrast, must first be phosphorylated to its monophosphate form and then binds at the substrate binding site, inducing a closed conformation of the enzyme that does not trap XMP (26).

We have shown that MPA induces a shift in IMPDH mobility in cell lines treated with the drug and that this shift is both prevented and reversed by the addition of guanosine to cell cultures, as well as by removal of the MPA from the medium. Since a similar shift occurs when the purified protein is incubated with drug in the presence of IMP and NAD^+ but is not found in cell lysates following mizoribine treatment (data not shown), we suggest that it results from the E-XMP intermediate bound to MPA. Recently, a similar mobility shift was reported for the yeast family of IMD enzymes (16) and conclusively shown to result from trapping of the covalently bound XMP intermediate in the presence of MPA. This shift was also reversible with the removal of MPA. These data support the conclusion that the shift results from a conformational change of the IMPDH protein, since the magnitude of the shift considerably exceeds the molecular weight increment of the E-XMP-MPA complex. We have now demonstrated the same shift of IMPDH in a mononuclear cell lysate from a patient receiving standard therapeutic doses of Mycophenolate mofetil (Fig. 1B). This alteration in gel mobility could provide a surrogate marker for IMPDH inhibition in clinical studies of drugs that bind to the NAD^+ binding site.

We have here demonstrated a unique consequence of IMPDH inhibition, the formation of large intracellular aggregates of protein that result in distinct annular configurations in the cytoplasm. These aggregates are formed in response to MPA, mizoribine, and VX-944, a new IMPDH inhibitor, in all cell types tested. They do not appear to involve any defined intracellular organelles either by immunocytochemical costaining techniques or by electron microscopy. Despite extensive investigation, we have not been able to identify any other interacting proteins in this complex. Finally, treatment of highly purified IMPDH protein with MPA *ex vivo* results in similar aggregation by both light and negative staining electron microscopy. Thus, this striking configuration of IMPDH appears to be a direct

function of an alteration in protein conformation. The ability of mizoribine to induce the ring-like aggregation of IMPDH in intact cells, but not to induce the gel mobility shift implies that the trapping of XMP is not required for this effect.

The ability of guanosine to reverse the effects of IMPDH inhibition has been well documented in numerous studies on the biologic sequelae of IMPDH inhibition (5,27,28) and has been used to prove that guanine nucleotide depletion is specifically responsible for the biologic effects of IMPDH inhibitors. We have now shown, however, that guanine nucleotides also reverse the conformational change induced in IMPDH by MPA treatment, both *in vivo* and *in vitro*. We have also shown that GTP itself can bind to IMPDH protein at physiologic concentrations. Although it is clear that GMP is a competitive inhibitor of IMPDH (29), the direct binding of GTP to IMPDH has not previously been demonstrated to our knowledge. We therefore hypothesize based on our microscopy studies that the IMPDH tetramer forms linear arrays by binding either ATP or GTP, putatively through the CBS domains. MPA, by causing conformational change in the protein and by reducing intracellular GTP levels, induces the formation of high molecular weight aggregates. The restoration of intracellular GTP levels reverses MPA-induced aggregation and restores enzymatic activity. The *in vitro* studies confirm that GTP not only reverses but also prevents IMPDH aggregation.

Although the specific physicochemical basis for these conformational changes has not been established, these studies indicate that the regulation of IMPDH by GTP levels may be important in the multitude of biologic effects of IMPDH inhibitors. Inhibition of IMPDH has been found to inhibit T and B cell activation (30), induce the differentiation of leukemic cell lines (31), cause apoptosis in hematopoietic and solid tumor cell lines (27,32), impair the maturation and function of dendritic cells (33), and interfere with glycosylation, cell adhesion and nitric oxide synthesis (34,35). The reversal of these important biologic effects by increasing intracellular GTP levels may be in part attributable to effects on IMPDH enzymatic activity and the restoration of *de novo* guanine nucleotide biosynthesis.

REFERENCES

1. Franchetti, P., and Grifantini, M. (1999) *Curr Med Chem* **6**, 599-614
2. Wright, D. G., Boosalis, M., Malek, K., and Waraska, K. (2004) *Leuk Res* **28**, 1137-1143
3. Kaur, R., Klichko, V., and Margolis, D. (2005) *AIDS Res Hum Retroviruses* **21**, 116-124
4. Robertson, C. M., Hermann, L. L., and Coombs, K. M. (2004) *Antiviral Res* **64**, 55-61
5. Zhou, S., Liu, R., Baroudy, B. M., Malcolm, B. A., and Reyes, G. R. (2003) *Virology* **310**, 333-342
6. Zimmermann, A. G., Gu, J. J., Laliberte, J., and Mitchell, B. S. (1998) *Prog Nucleic Acid Res Mol Biol* **61**, 181-209
7. Nagai, M., Natsumeda, Y., and Weber, G. (1992) *Cancer Res* **52**, 258-261
8. Zimmermann, A., Gu, J. J., Spsychala, J., and Mitchell, B. S. (1996) *Adv Enzyme Regul* **36**, 75-84
9. Gu, J. J., Spsychala, J., and Mitchell, B. S. (1997) *J Biol Chem* **272**, 4458-4466
10. Aherne, A., Kennan, A., Kenna, P. F., McNally, N., Lloyd, D. G., Alberts, I. L., Kiang, A. S., Humphries, M. M., Ayuso, C., Engel, P. C., Gu, J. J., Mitchell, B. S., Farrar, G. J., and Humphries, P. (2004) *Hum Mol Genet* **13**, 641-650
11. Sintchak, M. D., Fleming, M. A., Futer, O., Raybuck, S. A., Chambers, S. P., Caron, P. R., Murcko, M. A., and Wilson, K. P. (1996) *Cell* **85**, 921-930
12. McLean, J. E., Hamaguchi, N., Belenky, P., Mortimer, S. E., Stanton, M., and Hedstrom, L. (2004) *Biochem J* **379**, 243-251
13. Scott, J. W., Hawley, S. A., Green, K. A., Anis, M., Stewart, G., Scullion, G. A., Norman, D. G., and Hardie, D. G. (2004) *J Clin Invest* **113**, 274-284
14. Valentine, R. C., and Green, N. M. (1967) *J Mol Biol* **27**, 615-617
15. Northup, J. K., Smigel, M. D., and Gilman, A. G. (1982) *J Biol Chem* **257**, 11416-11423
16. McPhillips, C. C., Hyle, J. W., and Reines, D. (2004) *Proc Natl Acad Sci U S A* **101**, 12171-12176
17. Allison, A. C., and Eugui, E. M. (1993) *Immunol Rev* **136**, 5-28
18. Picard, N., Ratanasavanh, D., Premaud, A., Le Meur, Y., and Marquet, P. (2005) *Drug Metab Dispos* **33**, 139-146
19. Kerr, K. M., and Hedstrom, L. (1997) *Biochemistry* **36**, 13365-13373
20. Nimmesgern, E., Fox, T., Fleming, M. A., and Thomson, J. A. (1996) *J Biol Chem* **271**, 19421-19427
21. Behrend, M. (1996) *Clinical Nephrology* **45**, 336-341
22. Pankiewicz, K. W., Patterson, S. E., Black, P. L., Jayaram, H. N., Risal, D., Goldstein, B. M., Stuyver, L. J., and Schinazi, R. F. (2004) *Curr Med Chem* **11**, 887-900
23. Picardi, A., Gentilucci, U. V., Zardi, E. M., D'Avola, D., Amoroso, A., and Afeltra, A. (2004) *Curr Pharm Des* **10**, 2081-2092
24. Ishikawa, H. (1999) *Curr Med Chem* **6**, 575-597
25. Colby, T. D., Vanderveen, K., Strickler, M. D., Markham, G. D., and Goldstein, B. M. (1999) *Proc Natl Acad Sci U S A* **96**, 3531-3536

26. Kohler, G. A., Gong, X., Bentink, S., Theiss, S., Pagani, G. M., Agabian, N., and Hedstrom, L. (2005) *J Biol Chem* **280**, 11295-11302
27. Gu, J. J., Gathy, K., Santiago, L., Chen, E., Huang, M., Graves, L. M., and Mitchell, B. S. (2003) *Blood* **101**, 4958-4965
28. Jonsson, C. A., and Carlsten, H. (2001) *Clin Exp Immunol* **124**, 486-491
29. Gilbert, H. J., Lowe, C. R., and Drabble, W. T. (1979) *Biochem J* **183**, 481-494
30. Dayton, J. S., Lindsten, T., Thompson, C. B., and Mitchell, B. S. (1994) *J Immunol* **152**, 984-991
31. Li, W., and Weber, G. (1998) *Life Sci* **63**, 1975-1981
32. Messina, E., Barile, L., Lupi, F., and Giacomello, A. (2004) *Nucleosides Nucleotides Nucleic Acids* **23**, 1545-1549
33. Mehling, A., Grabbe, S., Voskort, M., Schwarz, T., Luger, T. A., and Beissert, S. (2000) *J Immunol* **165**, 2374-2381
34. Allison, A. C., and Eugui, E. M. (2000) *Immunopharmacology* **47**, 85-118
35. Srinivas, T. R., Kaplan, B., and Meier-Kriesche, H. U. (2003) *Expert Opin Pharmacother* **4**, 2325-2345

FOOTNOTES

This work was supported by NIH grant RO-1 CA64192. Y. Ji was supported as a Rothrock Thomas fellow. Electron microscopy studies were supported by grants CA16086 and GM31819 (to J.D.G). We would like to thank Jozef Sychala for the critical reading of the manuscript.

The abbreviations used are: Hypoxanthine-guanine phosphoribosyl transferase (HGPRT); Inosine monophosphate dehydrogenase (IMPDH); Mycophenolic acid (MPA); Inosine monophosphate (IMP); Guanosine (G); 6-thioguanine (6-TG); Chronic myelogenous leukemia (CML).

FIGURE LEGENDS

Figure 1. Effects of IMPDH inhibitors on IMPDH and reversal by guanosine. (A) Western blot of MCF7 cell lysate after treatment with ethanol (lane 1); 2 μ M MPA plus 100 μ M guanosine for 24 h (lane 2); or MPA for 5 min (lane 3), 2 h (lane 4), or 24 h (lane 5). IMPDH type I (I) and IMPDH type II (II) are indicated. The arrow shows the shifted XMP-IMPDH intermediate. (B) Mononuclear cells obtained from a normal volunteer (lane 1) and from a patient treated with CellCept (lane 2). (C) Lysate from MCF7 cells untreated (lane 1) or treated with MPA in the absence (lane 2) or presence (lanes 3-4) of 100 μ M guanosine. Guanosine was added for the entire 60 min incubation period (lane 3) or for the final 10 min (lane 4). In lane 5, after 1 h MPA treatment, cells were washed twice in medium, and incubated for an additional 60 min in the absence of drug. (D) Effect of MPA and guanosine on IMPDH activity. MCF7 cells were incubated in the presence of 2 μ M MPA (M) for 24 h. 100 μ M guanosine (G) was added for the final 30 min, 60 min, or 90 min. The cells were then processed and assayed for IMPDH activity, as indicated in Experimental Procedures. Data are shown as the mean \pm SEM of at least three determinations.

Figure 2. Effects of MPA on IMPDH aggregation and localization in intact cells. (A) Immunofluorescent staining of intracellular IMPDH in MCF7 cells treated with 2 μ M MPA for 30 min, 2 h, or 24 h. (B) Immunofluorescent staining of IMPDH after 24 h MPA treatment in MCF7 cells. Visualization with confocal microscopy was performed at a magnification of 630x.

(C) Electron micrographs of MCF7 cells treated with MPA for 24 h. Cells were stained with IMPDH specific Ab and visualized with a secondary Ab conjugated with nanogold particles, as outlined in Experimental Procedures.

Figure 3. Effects of guanosine and GTP on IMPDH aggregation and activity in cells. (A) HGPRT⁻ CEM cells or (B) HGPRT⁻ K6H6/B5 cells were treated with MPA for 16 h. Guanosine (100 μ M) or GTP (1 mM) was added for the final 2 h of culture. (C) MCF7 (HGPRT⁺) cells were treated with 2 μ M MPA for 24 h and with Guanosine (100 μ M) or non-hydrolyzable GTP γ S (1 mM) for the last 60 min. (D) IMPDH activity in untreated MCF7 cells for 24 h (1), cells treated for 24 h with 2 μ M MPA alone (2) or with 24 h MPA and GTP γ S for the final 1 h (3). Data represent the mean \pm SEM of three determinations.

Figure 4. Effect of MPA in inducing aggregation of IMPDH. (A) Gel filtration of MCF7 cell lysate obtained from cells treated in the absence or presence of MPA for 6 h. Relative IMPDH levels were examined by Western blot followed by densitometry of the 55 kDa subunit band. (B) Immunostaining of purified IMPDH protein untreated or treated with 2 μ M MPA for 10 min. Protein was spread on poly-lysine coated slides and visualized by fluorescent microscopy at a magnification of 1000x.

Figure 5. Electron micrographs of purified IMPDH protein treated with MPA in the absence or presence of nucleoside triphosphates. Samples were prepared as indicated in Experimental Procedures. IMPDH protein at a concentration of 50 μ g/ml was incubated with ethanol vehicle (A), 1 mM GTP (B), or 2 mM ATP (C) for 15 min at RT. Panels D-F show IMPDH protein after treatment with 2 μ M MPA for 15 min. Protein was then incubated for an additional 15 min with water (D), 1 mM GTP (E), or 2 mM ATP (F). The inserts represent higher magnifications of individual or dimeric tetramers (A) or chains of tetramers (B, C and E). Scale bar represents 100 nm for A-F; 42 nm for inserts in B, C, F and 25 nm for inserts in A.

Figure 6. Schema of structural alterations of IMPDH induced by MPA and nucleotides.

Figure 7. Dissociation of GTP from IMPDH. IMPDH was incubated with a fixed concentration of [α -³²P]GTP and increasing concentrations of cold GTP for 10 min at RT. The reaction mixtures were loaded on MF filter membranes under vacuum. After washing, the radioactivity bound to the filter was measured by scintillation counting. Data were plotted using SigmaPlot and fitted to a four parameter logistic curve. The Kd value is the mean \pm SEM of 3 determinations.

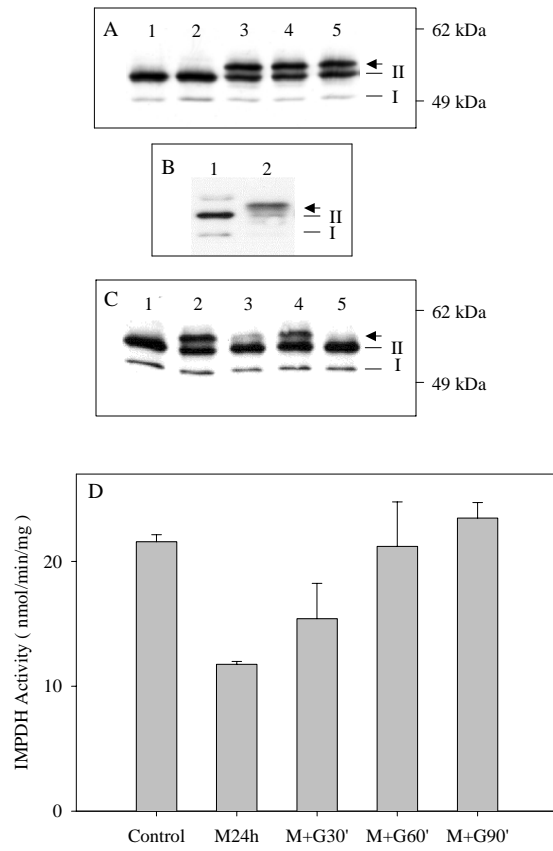


Figure 1

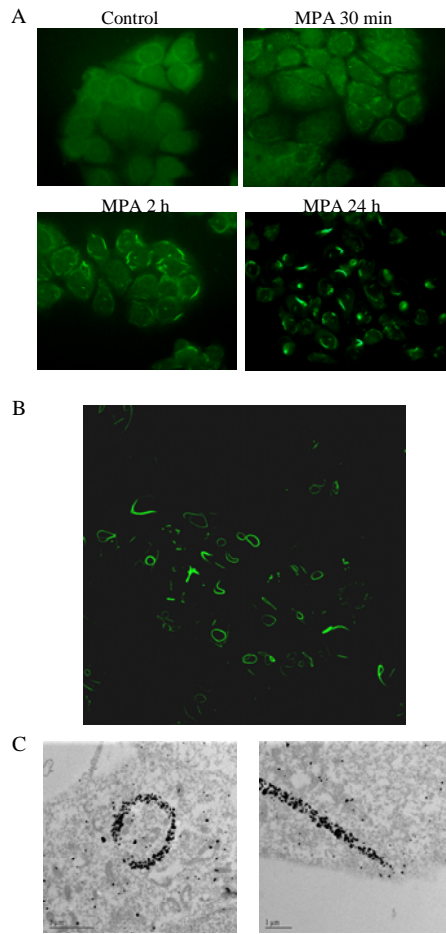


Figure 2

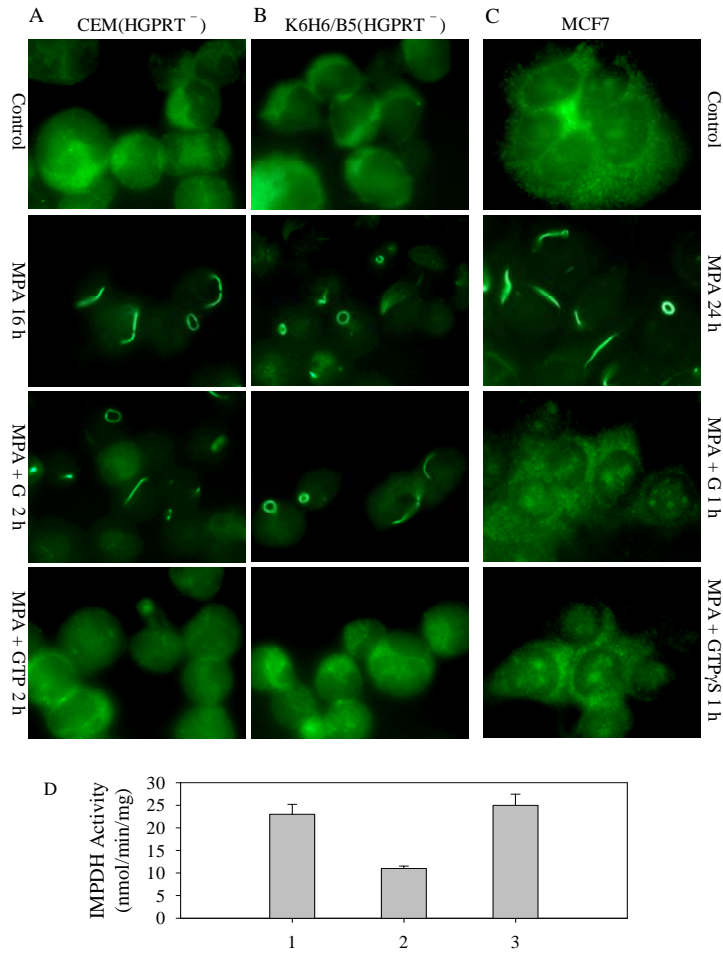


Figure 3

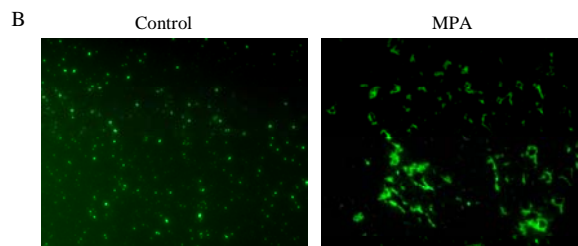
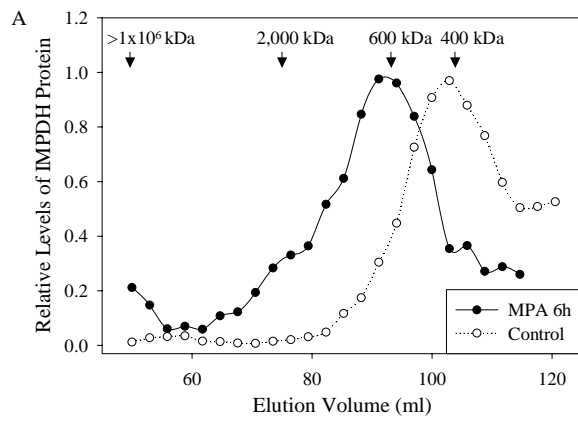


Figure 4

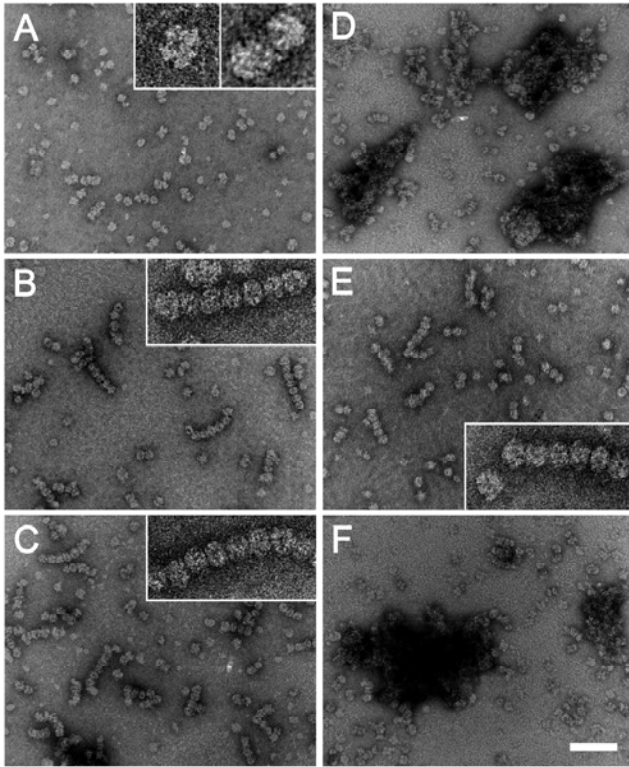


Figure 5

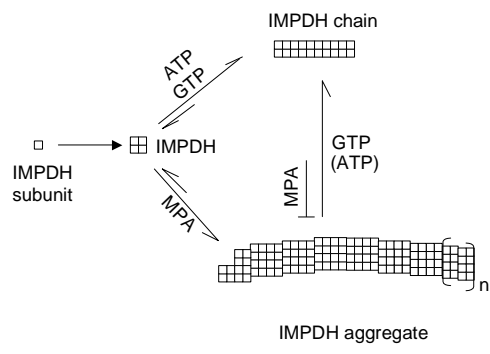


Figure 6

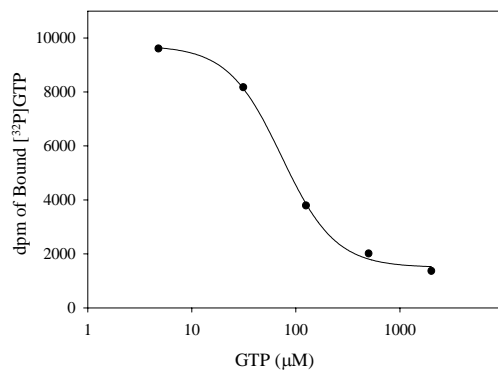
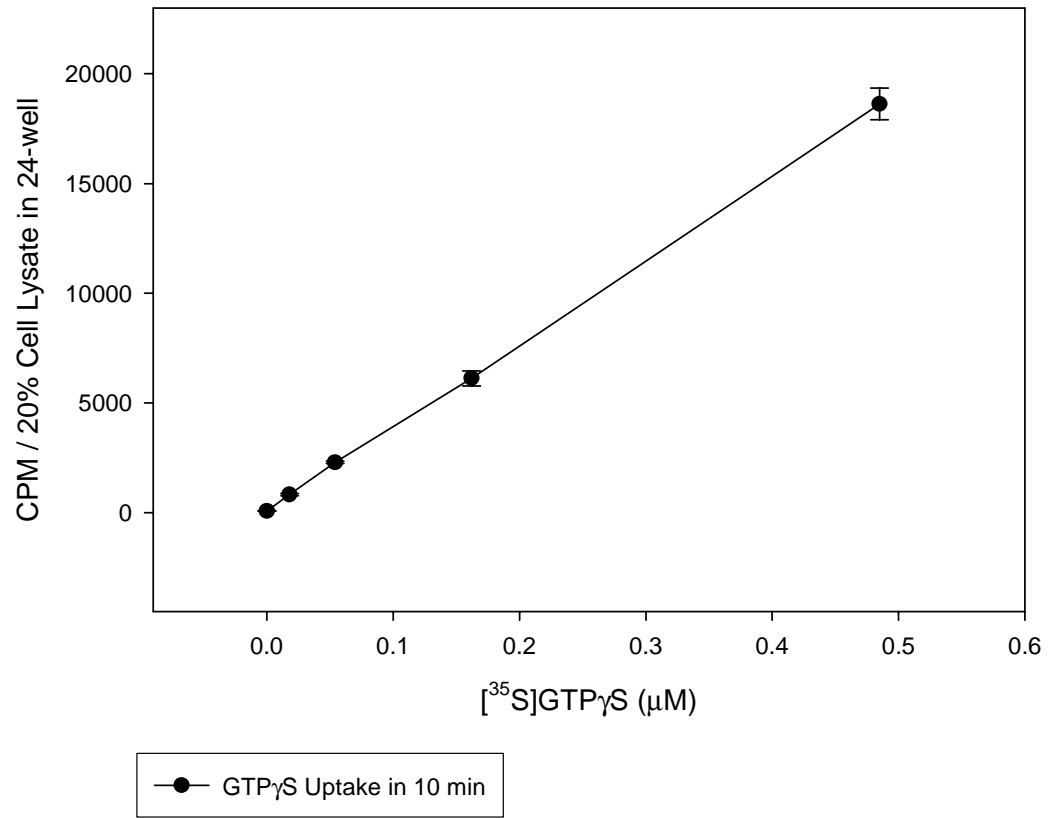
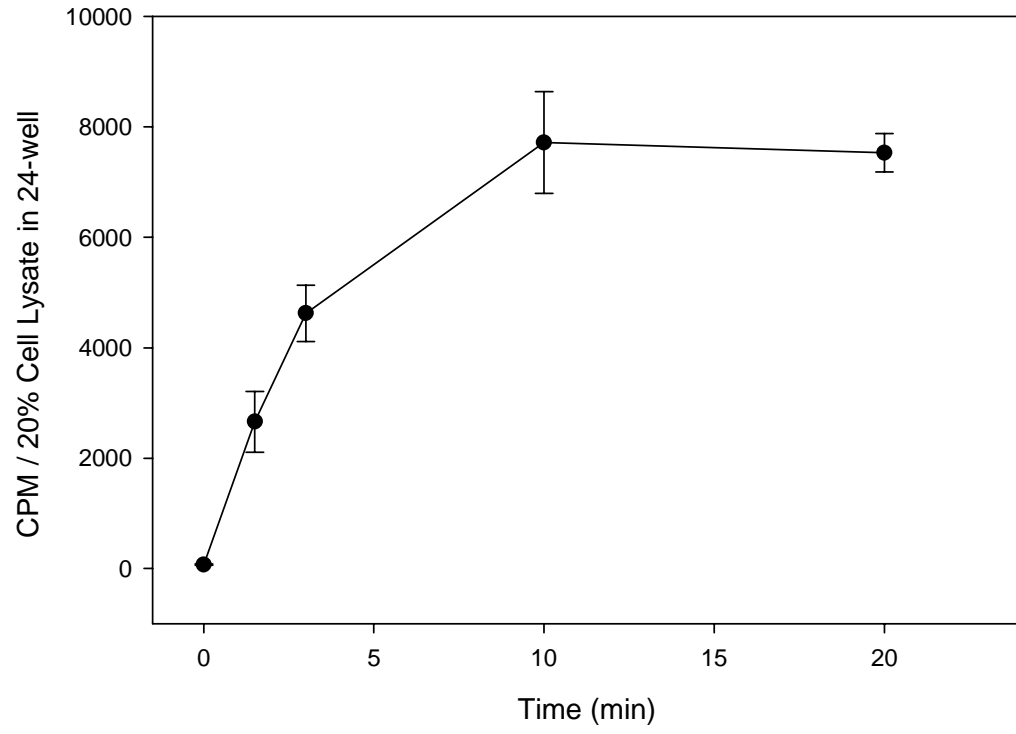


Figure 7

Dose Response of GTP γ S Uptake into MCF7 Cells



[³⁵S]GTPγS Uptake into MCF7 Cells



10μCi(0.2μM)GTPγS / well